Hindawi
International Journal of Polymer Science
Volume 2020, Article ID 9209108, 10 pages
https://doi.org/10.1155/2020/9209108

Research Article

Starch-Based Fishing Composite Fiber and Its Degradation Behavior

Wenwen Yu,[1] **Fei Yang**,[2] **Lei Wang**,[1] **Yongli Liu**,[1] **and Jiangao Shi**[1]

[1]*East China Sea Fisheries Research Institute, Chinese Academy of Fishery Sciences, Shanghai 200090, China*
[2]*Guangdong Overseas Fisheries Association, Guangzhou 510240, China*

Correspondence should be addressed to Jiangao Shi; jiangaoshi666@163.com

Received 29 July 2020; Revised 9 October 2020; Accepted 15 October 2020; Published 30 October 2020

Academic Editor: José Luis Rivera-Armenta

The starch-based fishing composite fibers were prepared by one-step reactive extrusion and melt spinning. The effects of starch contents on the microstructural, thermal, dynamic mechanical, and mechanical properties of starch-based composite fibers were studied. And the degradation behaviors in soil of the fibers were also investigated. The compatibility between starch and HDPE is improved significantly by grafting maleic anhydride (MA) using one-step reactive blending extrusion. As the starch content increased, the melting temperature and the crystallinity of the fibers gradually decreased due to fluffy internal structures. Dynamic mechanical analysis showed that the transition peak α in the high-temperature region was gradually weakened and narrowed with increasing starch content; moreover, a shoulder appeared on the low-temperature side of the α peak was assigned to the β-relaxation related to starch phase. In addition, the mechanical results showed the significant decrease in the breaking strength and increase in the elongation at break of the starch-based composite fibers as the starch content increased. After degradation in soil for 5 months, the surface of the composite fibers had been deteriorated, while flocculent layers were observed and a large number of microfibers appeared. And the weight loss rate of the starch-based composite fibers (5.2~34.8%) significantly increased with increasing starch content (50~90 wt%).

1. Introduction

Abandoned, lost, and discarded fishing gears (ALDFGs), also known as "ghost fishing" gear, can cause considerable ecological and economic losses [1]. Due to the continuous growth of fisheries and the transformation of fishing gear materials from natural materials (e.g., wood and cotton) to poorly degradable synthetic materials (e.g., polyethylene, polypropylene, nylon, and polyester), the amount, distribution, and environmental impact of ALDFGs have significantly increased over the last few decades [2, 3]. Some researchers indicate that about 640 t of fishing gear is lost in the ocean every year [4]. Indeed, white pollution and ghost fishing caused by nonbiodegradable fishing gear have attracted wide attention as public environmental awareness and requirements for environmental quality have improved [5, 6]. Thus, the research on the environment-friendly and biodegradable fishing materials has become an important means to protect the marine ecological environment and prevent ALDFGs from causing harm to marine life.

Starch has attracted considerable attentions due to its natural abundance, low cost, and complete biodegradability [7–11]. Unfortunately, the mechanical properties and hydrophobicity of starch materials are poorer than those of synthetic plastics. Some authors have tried to overcome these weaknesses by blending starch with a polymer with good mechanical properties, while maintaining the biodegradability of the product [12–16]. Raquez et al. [17] have focused on the grafting of maleic anhydride (MA) onto the polymeric backbone using reactive extrusion methods. Such reactions promoted by MA moieties reduced the intrinsic viscosity of the blends, expecting an improvement in its processability. Pervaiz et al. [18] found that water absorption was reduced significantly after blending starch facilitated with green polyethylene and MA by reactive extrusion. Reactive extrusion is the simplest and most cost effective method for carrying out this reaction. The grafted MA can react with the hydroxyl

groups of starch macromolecules to form covalent bonds, and thus, they provide better control of the size of phase and strong interfacial adhesion and improve the stress transfer between the component phases [17, 19]. Researchers in the past have reported the modified starch foams [20], films [21, 22], and molding products; however, rare studies are found on starch-based fiber or monofilament, which is required for fishing net and rope.

In this current work, we attempt to prepare starch-based composite fibers using plasticized cassava starch and high-density polyethylene (HDPE) via one-step reactive extrusion with maleic anhydride (MA) and the melt spinning method. The grafting MA is expected to influence remarkably the microstructure, thereby leading to the changes in properties. In view of the fact that starch content is one of the important factors that strongly influence the morphology and properties of blends [15, 16, 20–23], we try to design composite fibers with different starch content to examine the effect of starch content on the physicochemical parameters and soil degradation for composite fibers.

2. Materials and Methods

2.1. Materials. Plasticized cassava starch (STR) was obtained from Zhangjiakou Yujing Starch Factory. The thermoplastic cassava starch was prepared by blending with cassava starch, low-density polyethylene (LDPE), plasticizer, and glycerol. The weight ratio of starch/LDPE is 9, and its density was 1500 kg/m^3. HDPE (5000S) with an MFI 0.9 g per 10 min and density 950 kg/m^3 was supplied by Sinopec Yangzi Petrochemical Company, China. Maleic anhydride (MA) was purchased from Sigma-Aldrich (Shanghai) Trading Co., Ltd. Dicumyl peroxide (DCP) and soybean oil were obtained from Shanghai Chemical Reagent Company, China Pharmacy Group.

2.2. Preparation of Starch-Based Fishing Composite Fibers by One-Step Reactive Extrusion. Plasticized cassava starch, HDPE (according to the experimental formulations shown in Table 1), MA, DCP, and soybean oil were added to premix, and then the mixture extruded in a twin-screw extruder for melt blending. MA and DCP were used as monomer and initiator at the 2.5 wt% and 0.25 wt% level based on starch. The temperatures of zones ①, ②, ③, ④, ⑤, ⑥, and ⑦ in the extruder were 130, 148, 155, 160, 160, 160, and 160°C, respectively. The twin-screw aspect ratio was 1 : 28, and the screw speed was 250 rpm corresponding to a mean residence time of around 5 min. Starch and HDPE were combined by reactive blending with MA agents during the melt extrusion process (Scheme 1). Then, the mixture was extruded from the spinneret. The diameter of the spinneret was 1 mm. The extruded as-spun fibers were drawn three times, and the total drawing ratio is 7.5-8, under which the composite monofilaments are continuously melt-spun. The temperatures of the draft water bath were 95, 98, and 98°C. The starch-based composite fibers were obtained by winding up the melt spinning tow with a reeler. Plasticized cassava starch was added to the starch-based composite fiber systems at proportions of 0 wt%, 50 wt%, 80 wt%, and 90 wt% and designated as HDPE, STR-50, STR-80, and STR-90, respectively (Table 1). For comparison purposes, the STR/HDPE fiber (50 wt% starch and 50 wt% HDPE) without adding MA was prepared in the same way.

Table 1: Composition of starch-based composite fibers.

Samples	Starch weight (wt%)	HDPE weight (wt%)
HDPE	0	100
STR-50	50	50
STR-80	80	20
STR-90	90	10

2.3. Soil Degradation of Starch-Based Composite Fibers. Starch-based composite fibers were dried in an oven at 80°C for 48 h and then weighed (M_0). Next, the composite fibers were buried 10 cm under the surface of the soil for 5 months. The soil humidity is 20%. The fibers were retrieved and then soaked into purified water for 24 h. After washing with purified water, the samples were dried at 80°C for 48 h and weighed (M_d). The weight loss rate of the fibers was calculated according to Equation (1).

$$\text{Weight loss rate}\,(\%) = \frac{M_0 - M_d}{M_0} \times 100\%. \quad (1)$$

2.4. Characterization. SEM instrument (S4800, JEOL Ltd., Japan) was used to observe the surface and fractural morphologies of the composite fibers. Here, the surface of each sample was completely dried, quenched with liquid nitrogen, and sprayed with gold. The sample was then fixed on the sampling stage using conductive glue and placed in the observation chamber of the scanning electron microscope for imaging.

Differential scanning calorimetry (DSC) was applied to investigate the melting and crystallization behavior of the monofilaments using the DSC thermal analyzer (204F1, Netzsch Instruments, Germany). The sample was heated from 0°C to 150°C at a rate of 10°C/min, and the nitrogen flow was set to 50 mL/min.

The crystallinity (X_c) of the samples was calculated according to Equation (2).

$$X_c = \left(\frac{\Delta H_f^{\text{obs}}}{\Delta H_f^{0}}\right) \times 100, \quad (2)$$

where ΔH_f^{obs} is the measured enthalpy of melting, ΔH_f^{0} is the enthalpy of melting of the completely crystalline polymer, and ΔH_f^{0} is the enthalpy of melting of HDPE (293 J/g) [24].

Dynamic mechanical analysis (DMA) was used as a mode of tensile clamp (242C, Netzsch Instruments, Germany) under the frequency of 1 Hz and the amplitude of 30 μm for all samples. During analysis, the temperature was increased from −184°C to 150°C at a rate of 3°C/min.

The tensile properties were investigated using the electron tensile tester (4466, Instron Instruments, USA) at a crosshead speed of 300 mm/min on a 500 mm long specimen

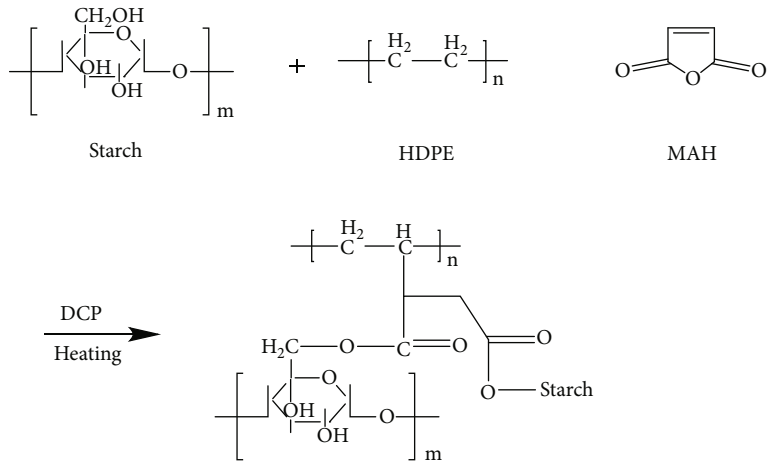

Scheme 1: Schematic representation of synthesis procedure for MA grafting STR/HDPE.

according to SC/T 5005-2014 under ambient conditions. Results are the average of at least 10 specimens.

Fourier transform infrared (FT-IR) spectroscopy was conducted to characterize the microstructures of the starch-based composite fibers (6700, Nicolet Instrument, USA). For the attenuated total reflectance (ATR), an additional solid probe system was applied. The samples were scanned over the wavenumber range of 700–4000 cm^{-1} at a resolution of 4 cm^{-1}.

3. Results and Discussion

3.1. Morphological Structure of Starch-Based Composite Fibers. Figure 1 shows the FT-IR spectra of the composite fibers with different starch contents. There were three characteristic peaks of starch, with those at 1110 cm^{-1} and 1157 cm^{-1} attributed to C–O–H bond stretching, and that near 1025 cm^{-1} attributed to the stretching vibration of C–O in C–O–C groups [22, 25]. It can be seen that these absorption peaks are not detected in the FT-IR spectra of HDPE, so these peaks belong to starch, and the characteristic peak intensity gradually increases with the increase of starch content. Strong absorption peaks were observed near 2916, 2848, and 1460 cm^{-1}, which could be, respectively, assigned to symmetrical and asymmetry stretching vibration of C–H bonds, bending vibration of C–H bonds [26]. With the increase of starch content, the content of HDPE in the composite fiber decreased, and these absorption peaks strength decreased significantly. Compared to STR/HDPE fiber without MA, the –C=O stretching vibration peak was observed at 1720 cm^{-1} for composite fibers with grafting MA due to esterified starch by MAH. The characteristic peak at 1270 cm^{-1} represents C–O in the O–C=O bonds present in the ester structure [27]. For the STR/HDPE fiber without MA, a relevant band from 3200 to 3400 cm^{-1} could be observed due to the stretching of inter- and intramolecular bonding hydroxyl groups of granular starch [17]. When MA was used as a grafting agent, weak peaks at 3200 to 3400 cm^{-1} appeared due to the reaction between starch and MA groups.

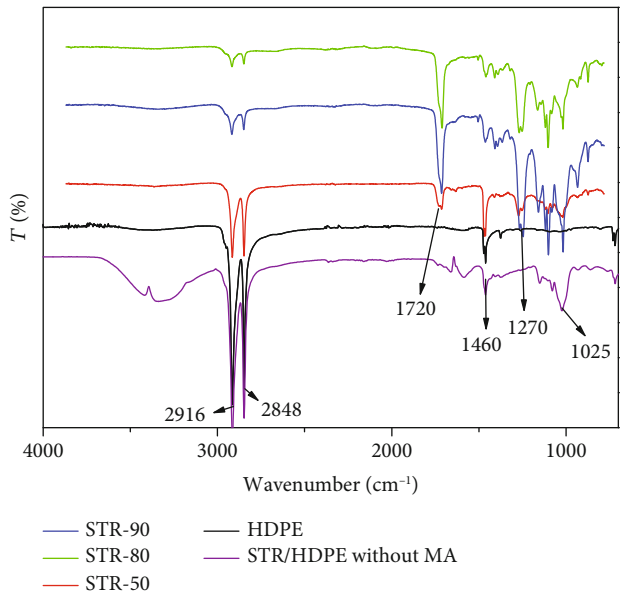

Figure 1: FT-IR spectrum of starch-based composite fibers.

It is necessary to study the morphology of composite fibers since many properties depend on it. SEM images of the starch-based composite fibers are shown in Figure 2. The STR/HDPE fiber without grafting MA displayed an obvious phase separation phenomenon (Figure 2(b)). The starch particles were not completely demolished and some of them were removed from the surface of the fiber during the fracture of the specimen, leaving some cavities in the fracture surface. The interfacial adhesion between starch and HDPE was poor due to the structural difference of dissimilar polymers [18]. However, after adding MA, the sample revealed a homogeneous fractural surface and compact structure (Figures 2(c) and 2(d)). There was no apparent phase interface between starch and HDPE in STR-50. Thereby, the compatibility between starch and HDPE is improved significantly by grafting MA using one-step reactive extrusion.

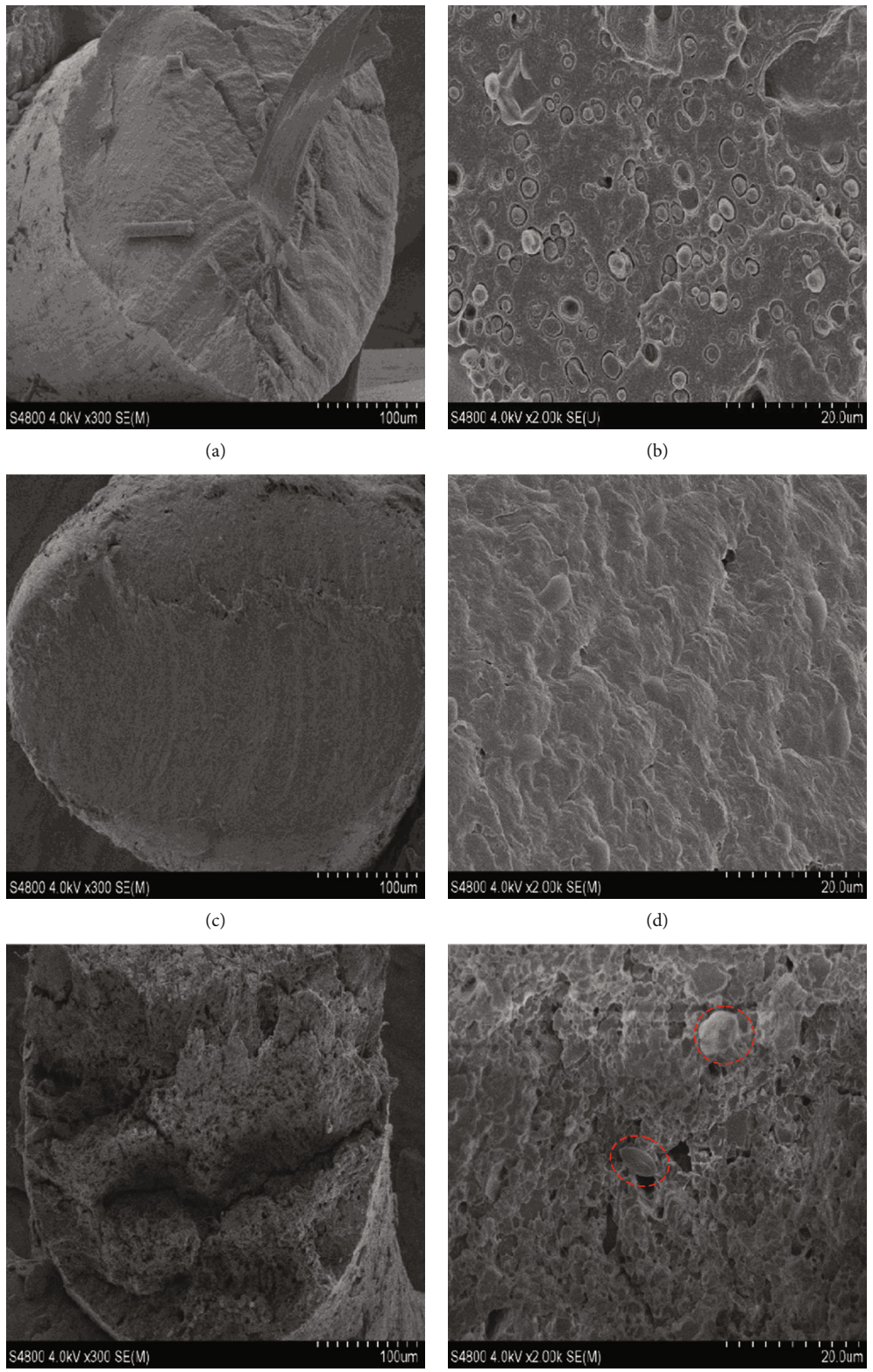

Figure 2: SEM images of starch-based composite fibers. (a) STR/HDPE fiber without adding MA at 300x. (b) STR/HDPE fiber without adding MA at 2000x. (c) STR-50 at 300x. (d) STR-50 at 2000x. (e) STR-90 at 300x. (f) STR-90 at 2000x.

This indicated that the compatibility of the composite fibers with adding MA was improved. However, it was noted that the internal structure of the composite fibers gradually became fluffy as the starch content increased (Figures 2(e) and 2(f)). As the starch content of the samples increased, the starch granules were congregated during the plasticization extrusion to become agglomerates. The presence of starch granules was attributed to the interaction of hydrogen bonds between molecules.

3.2. Thermal Properties of Starch-Based Composite Fibers. DSC thermograms were used to analyze the thermal properties of the starch-based composite fibers, and the results are shown in Figure 3. X_c of polyethylene in the composite fiber samples was calculated by the melting enthalpy, as shown in Figure 4. The melting temperature (T_m) of polyethylene in the starch-based composite fibers gradually decreased, thus improving the processability of the STR/HDPE composites. Importantly, the X_c of the samples decreased, and the crystal melting peak narrowed as the starch content increased. Compared to pure HDPE, the X_c of STR-80 decreased by 53.9%. This is because the introduction of starch reduces the order of polyethylene and destroys the crystal perfection of polyethylene, resulting in a decrease in the crystallinity and T_m of polyethylene as the starch content of the composite fibers increases. In addition, it was noted that the DSC curve of HDPE and STR-50 had only one heat absorption peak, but STR-80 and STR-90 showed another inflection point at about 96°C. It is speculated that the absorption peak is the endothermic peak of starch gelatinization, which is caused by the double conversion of starch gelatinization from polycrystalline state to amorphous state and from granular state to gelatinization state [28].

3.3. Dynamic Mechanical Properties of Starch-Based Composite Fibers. The dynamic mechanical properties of the starch-based composite fibers were studied, and the change curves of E' and tan δ of the fibers were obtained at temperatures ranging from −184°C to 150°C (Figure 5). Results showed that E' of the starch-based composite fibers significantly decreased compared with that of HDPE fibers. When the temperature was 30°C, E' of the STR-90 was 0.1 GPa, indicating a decrease of 79% compared with that of pure HDPE (Figure 5(a)). The transition peaks α and γ of HDPE and the starch-based composite fibers were detected over a wide range of temperatures; here, the transition peak γ at the low-temperature region corresponds to the glass transition peak of polyethylene [29–31]. The peak temperature of γ remained essentially unchanged with increasing starch content, thus indicating that the effect of starch content on glass transition is not significant.

The transition peak α at the high-temperature region is related to the movement of restricted segments near the crystal region of polyethylene and a complex multiple relaxation, which gradually weakens and narrows as the starch content increases. Moreover, with increasing starch content, the α peak transition of composite fibers moved to lower temperature. The DSC results showed that the X_c of the composite fibers decreased and their crystal melting peak narrowed as

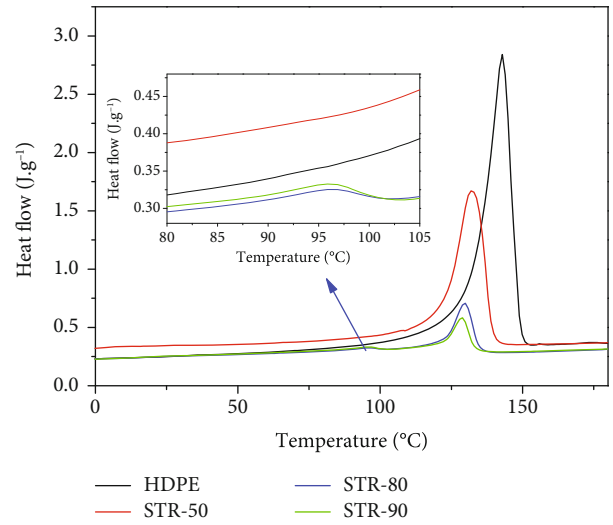

Figure 3: DSC analysis curves of starch-based composite fibers.

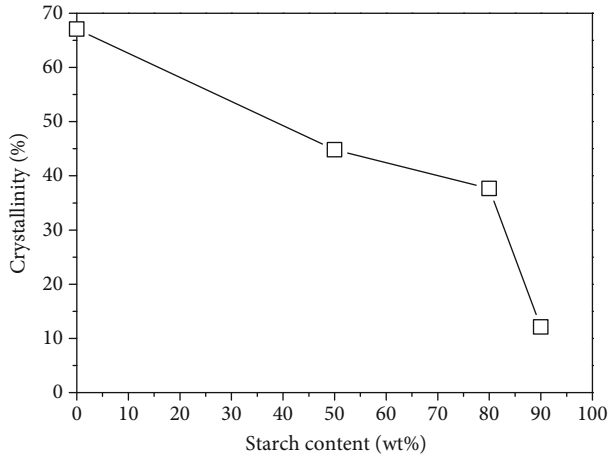

Figure 4: The X_c of polyethylene for starch-based composite fibers.

their starch content increased. Therefore, restricted segments near the polyethylene crystalline region decreased, consistent with the results of Abdul Wahab et al. [32]. It was noted that STR-80 and STR-90 revealed three transition peaks, while HDPE and STR-50 revealed two transition peaks. A shoulder appeared on the low-temperature side of the α peak. The shoulder in the DMA curves of the composites was assigned to the β-relaxation related to the starch phase, consistent with the results of our previous study [33]. The α and β peaks of STR-50 merged into one peak, thereby indicating that the compatibility of the composite fibers is improved when the starch content is 50 wt%. The result was in agreement with SEM analysis.

3.4. Mechanical Properties of Starch-Based Composite Fibers. Figure 6 shows the mechanical properties of HDPE and starch-based composite fibers. Compared to pure HDPE fiber, the breaking strength of the starch-based composite fibers significantly decreased. Importantly, with increasing

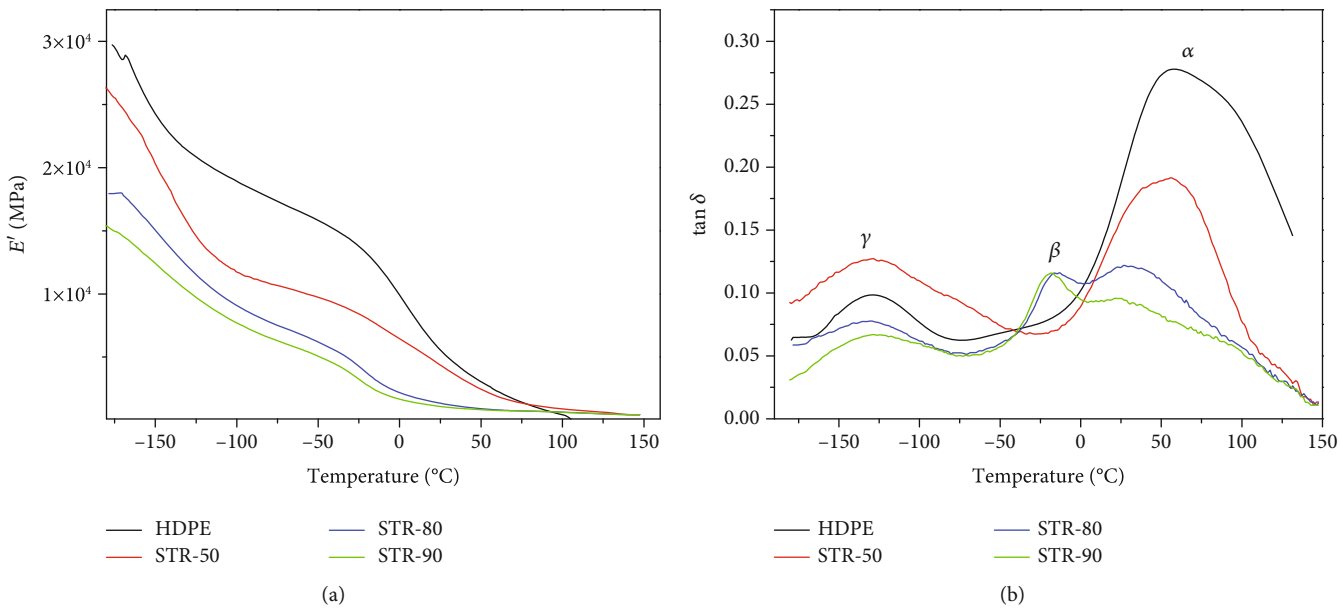

Figure 5: Starch-based composite fibers (a) E' and (b) tan δ vs. temperature.

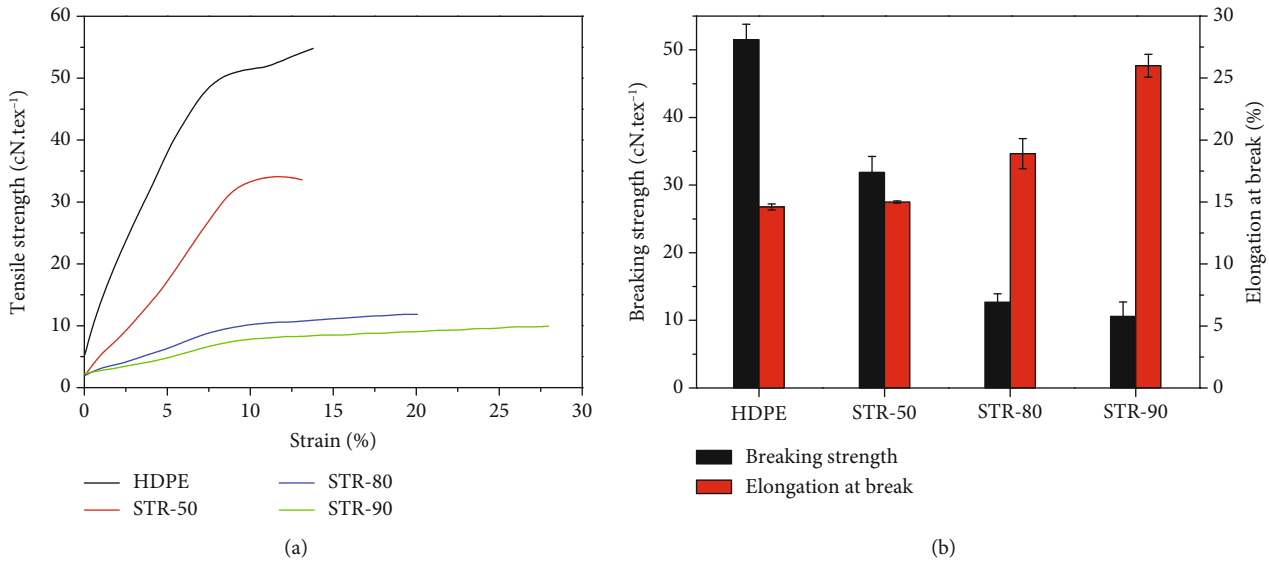

Figure 6: (a) Tensile strength-strain curves and (b) breaking strength and elongation at break of starch-based composite fibers.

the starch contents, the notable decrease in breaking strength and the increase in elongation at break can be observed in the starch-based composite fibers. Such a phenomenon was also reported in HDPE/starch blends in our previous study [33]. Differences between the tensile strength and elongation at break of the samples can be discussed in terms of their morphologies [34]. On increasing the content of starch, the mechanical properties worsened dramatically, especially the tensile strength for samples STR-80 and STR-90. This is ascribed to their internal structure became fluffy and the presence of starch granules. These features may form a stress concentration region, resulting in a significant decrease in mechanical properties of STR-80 and STR-90. Moreover, for the STR-80 and STR-90, it was clear that with the increase in starch contents, the length of the rubber plateau became longer (Figure 6(a)), which represented the typical pattern of rubbery starch plastic materials reported previously [35].

3.5. Soil Degradation Behavior of Starch-Based Composite Fibers

3.5.1. Effects of Soil Degradation on the Structural Morphology of Starch-Based Composite Fibers. SEM photographs demonstrated degradation of starch within the fibers; here, Figures 7(a) and 7(b) refer to the surface of STR-80 before and after soil degradation, respectively,

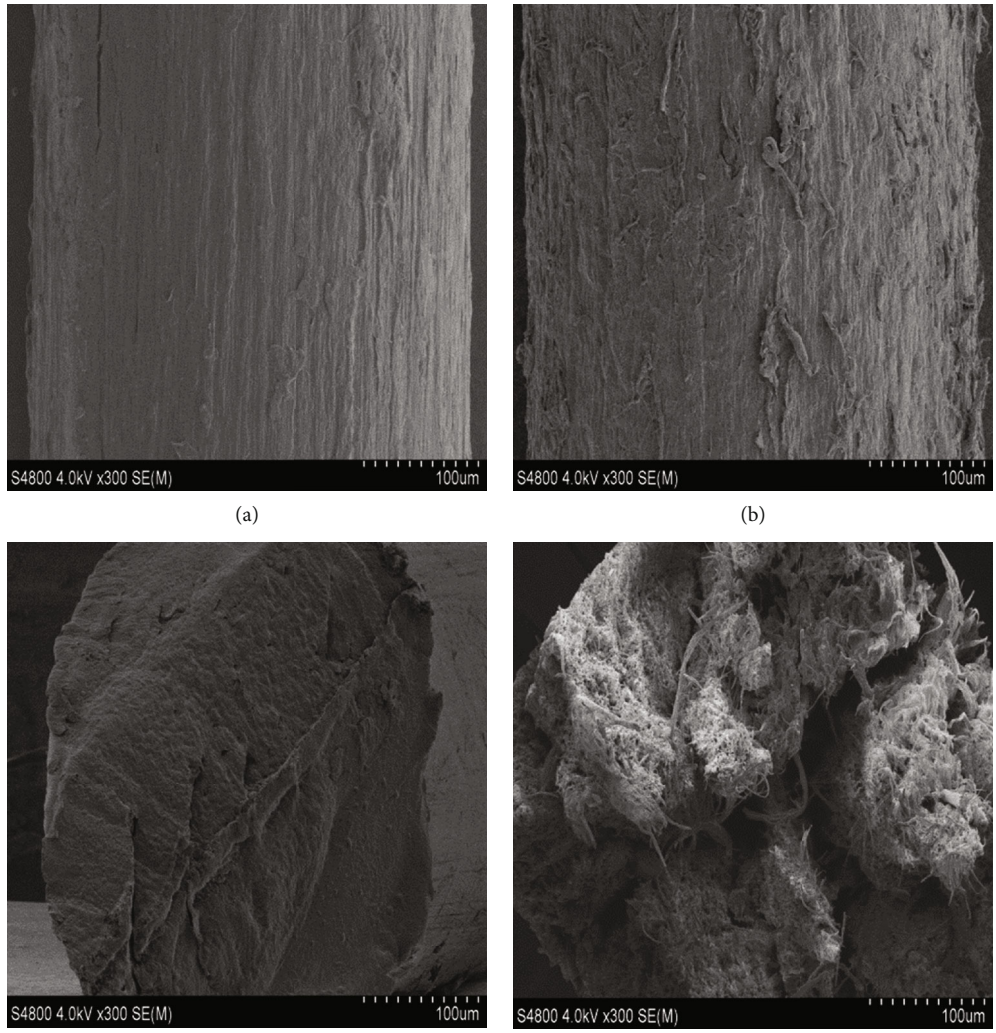

Figure 7: SEM images of starch-based composite fibers before and after biodegradation in soil. (a) Surface of STR-80 before soil degradation. (b) Surface of STR-80 after soil degradation. (c) Fractural structure of STR-80 before soil degradation. (d) Fractural structure of STR-80 after soil degradation.

while Figures 7(c) and 7(d) refer to the fractural section of the fiber sample before and after soil degradation, respectively. Before soil degradation, the surface of the composite fibers was smooth, no evident delamination could be observed, and the internal structure was compact. After soil degradation, some flocculent layering can be found on the surface of the composite fiber (Figure 7(b)). Moreover, disintegration of starch brought about changes of the internal structure. Many filamentous flocculent and spongiform structures were observed on the fractural surface of the composite fiber (Figure 7(d)). The internal structure became collapsed after soil degradation, thus indicating that the starch-based composite fiber was eroded and degraded by microorganisms in the soil.

FT-IR was used to characterize microstructural changes in the starch-based composite fibers before and after soil degradation. Figure 8 shows the IR spectra of STR-50, STR-80, and STR-90 before and after soil degradation. After soil degradation, peak intensities of composite fibers after soil degradation at 2916 and 2848 cm^{-1} were both improved greatly. The increase in the intensity of these peaks was owing to the break of the polyethylene chain in degradation progress, which resulted in the increase in the terminal group numbers [36]. Moreover, the –C–O stretching vibration absorption peak near 1025 cm^{-1} was enhanced too. As indicated above, the band at 1025 cm^{-1} was attributed to the stretching vibration of C–O in C–O–C groups, and the degradation of starch led to the increase in the intensity of this peaks. Similar variations before and after degradation for starch/polyethylene film were reported by Wang et al. [22]. Hence, both starch and HDPE in the composite fibers exhibited varying degrees of degradation.

3.5.2. Weight Loss Rate of Starch-Based Composite Fibers. Figure 9 shows the rates of weight loss for the starch-based composite fibers after 5 months of soil degradation. The rates of weight loss for HDPE, STR-50, STR-80, and STR-90 were 0, 5.2%, 29.9%, and 34.8%, respectively. The weight loss rate

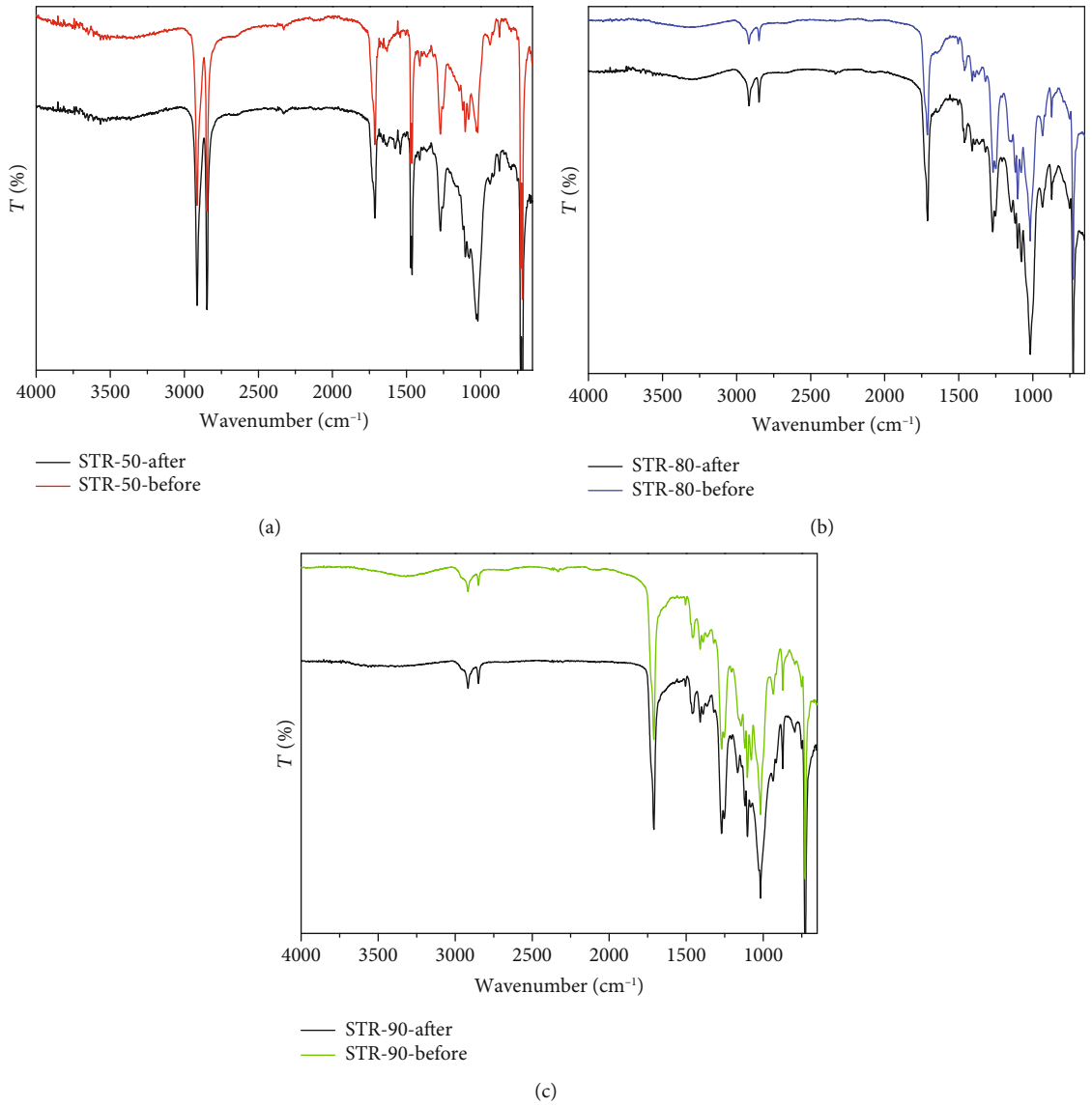

Figure 8: FT-IR spectrum of starch-based composite fibers before and after soil biodegradation.

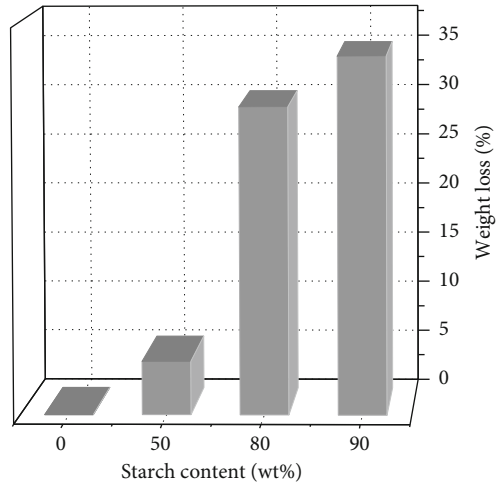

Figure 9: Weight loss of starch-based composite fibers after 5 months in soil degradation.

of the starch-based composite fibers significantly increased with increasing starch content. Starch fibers may be decomposed into oligomers, such as maltose and glucose, and, eventually, CO_2, H_2O, and other low-molecular weight compounds under the action of microorganisms. The presence of starch contributes to the multiplication of microorganisms that could easily destroy the structure and morphology of the composite fibers. FT-IR results showed that both starch and HDPE in the composite fibers exhibited varying degrees of degradation. However, the degradation of HDPE is only manifested as the break of the macromolecular chain but no weight loss. Bulatović et al. [37] found that thermoplastic starch was first degraded within the blend, which was facilitated access to the microorganisms of other ingredients in the blend, encouraging the biodegradation of other components. Although final values of weight loss are lower than expected in the composite fibers, indicating starch removal continues past 5 months.

4. Conclusions

Starch-based composite fibers were successfully prepared by one-step reactive extrusion and melt spinning technology. FT-IR and SEM data supported the fact that MA had been grafted as a potential compatibilizer for STR/HDPE systems. The STR/HDPE composite fibers with MA showed more homogeneous compared with the composite fibers without MA. The effect of starch contents on comprehensive morphological, thermal, and mechanical properties and soil degradation behavior was also studied. The starch contents had an important influence on the mechanical performance of the composite fibers due to the fluffy internal structure, the decrease of X_c, and small restricted segments near the crystalline region. In terms of soil degradation, SEM images of the polymers indicated surface deterioration. The weight loss rate of the composite fibers significantly increased with increasing starch content.

Data Availability

The data used to support the findings of this study are included within the article.

Conflicts of Interest

The authors declare that they have no conflicts of interest.

Acknowledgments

This study is supported by the National Natural Science Foundation of China (Nos. 31872611 and 31972844), the National Key R&D Program of China (No. 2019YFD0901505), the Ministry of Industry and Information Technology High Tech Ship Research Project (Engineering Development of Semi-submersible Agriculture Equipment), and is financially supported by the Marine S&T Fund of Shandong Province for Pilot National Laboratory for Marine Science and Technology (Qingdao) (No. 2018SDKJ0304-1).

References

[1] A. C. Correa, V. B. Carmona, J. A. Simão, L. H. Capparelli Mattoso, and J. M. Marconcini, "Biodegradable blends of urea plasticized thermoplastic starch (UTPS) and poly(ε-caprolactone) (PCL): morphological, rheological, thermal and mechanical properties," *Carbohydrate Polymers*, vol. 167, pp. 177–184, 2017.

[2] J. G. B. Derraik, "The pollution of the marine environment by plastic debris: a review," *Marine Pollution Bulletin*, vol. 44, no. 9, pp. 842–852, 2002.

[3] K. V. K. Gilardi, D. Carlson-Bremer, J. A. June, K. Antonelis, G. Broadhurst, and T. Cowan, "Marine species mortality in derelict fishing nets in Puget Sound, WA and the cost/benefits of derelict net removal," *Marine Pollution Bulletin*, vol. 60, no. 3, pp. 376–382, 2010.

[4] C. Wilcox, G. Heathcote, J. Goldberg, R. Gunn, D. Peel, and B. D. Hardesty, "Understanding the sources and effects of abandoned, lost, and discarded fishing gear on marine turtles in northern Australia," *Conservation Biology*, vol. 29, no. 1, pp. 198–206, 2015.

[5] E. Gilman, "Biodegradable fishing gear: part of the solution to ghost fishing and marine pollution," *Animal Conservation*, vol. 19, no. 4, pp. 320-321, 2016.

[6] S. Kim, P. Kim, J. Lim, H. An, and P. Suuronen, "Use of biodegradable driftnets to prevent ghost fishing: physical properties and fishing performance for yellow croaker," *Animal Conservation*, vol. 19, no. 4, pp. 309–319, 2016.

[7] J. B. Engel, A. Ambrosi, and I. C. Tessaro, "Development of biodegradable starch-based foams incorporated with grape stalks for food packaging," *Carbohydrate Polymers*, vol. 225, article 115234, 2019.

[8] H. A. Fonseca-Florido, F. Soriano-Corral, R. Yañez-Macías et al., "Effects of multiphase transitions and reactive extrusion on *in situ* thermoplasticization/succination of cassava starch," *Carbohydrate Polymers*, vol. 225, article 115250, 2019.

[9] M. Shayan, H. Azizi, I. Ghasemi, and M. Karrabi, "Influence of modified starch and nanoclay particles on crystallization and thermal degradation properties of cross-linked poly(lactic acid)," *Journal of Polymer Research*, vol. 26, no. 10, 2019.

[10] Z. B. Cuevas-Carballo, S. Duarte-Aranda, and G. Canché-Escamilla, "Properties and biodegradation of thermoplastic starch obtained from grafted starches with poly(lactic acid)," *Journal of Polymers and the Environment*, vol. 27, no. 11, pp. 2607–2617, 2019.

[11] N. G. Olaiya, I. Surya, P. K. Oke et al., "Properties and characterization of a PLA-chitin-starch biodegradable polymer composite," *Polymers*, vol. 11, no. 10, article 1656, 2019.

[12] Đ. Ačkar, J. Babić, A. Jozinović et al., "Starch modification by organic acids and their derivatives: a review," *Molecules*, vol. 20, no. 10, pp. 19554–19570, 2015.

[13] N. Castanha, D. C. Lima, M. D. Matta Junior, O. H. Campanella, and P. E. D. Augusto, "Combining ozone and ultrasound technologies to modify maize starch," *International Journal of Biological Macromolecules*, vol. 139, pp. 63–74, 2019.

[14] J. C. Cazotti, A. T. Fritz, O. Garcia-Valdez, N. M. B. Smeets, M. A. Dubé, and M. F. Cunningham, "Graft modification of starch nanoparticles using nitroxide-mediated polymerization and the grafting from approach," *Carbohydrate Polymers*, vol. 228, article 115384, 2020.

[15] S. M. Lai, C. K. Huang, and H. F. Shen, "Preparation and properties of biodegradable poly(butylene succinate)/starch blends," *Journal of Applied Polymer Science*, vol. 97, no. 1, pp. 257–264, 2005.

[16] J.-B. Zeng, L. Jiao, Y.-D. Li, M. Srinivasan, T. Li, and Y.-Z. Wang, "Bio-based blends of starch and poly(butylene succinate) with improved miscibility, mechanical properties, and reduced water absorption," *Carbohydrate Polymers*, vol. 83, no. 2, pp. 762–768, 2011.

[17] J. M. Raquez, Y. Nabar, M. Srinivasan, B. Shin, R. Narayan, and P. Dubois, "Maleated thermoplastic starch by reactive extrusion," *Carbohydrate Polymers*, vol. 74, no. 2, pp. 159–169, 2008.

[18] M. Pervaiz, P. Oakley, and M. Sain, "Extrusion of thermoplastic starch: effect of "green" and common polyethylene on the hydrophobicity characteristics," *Materials Sciences & Applications*, vol. 5, no. 12, pp. 845–856, 2014.

[19] J. W. Barlow and D. R. Paul, "Mechanical compatibilization of immiscible blends," *Polymer Engineering and Science*, vol. 24, no. 8, pp. 525–534, 1984.

[20] Y. Nabar, J. M. Raquez, P. Dubois, and R. Narayan, "Production of starch foams by twin-screw extrusion: effect of maleated poly(butylene adipate-*co*-terephthalate) as a compatibilizer," *Biomacromolecules*, vol. 6, no. 2, pp. 807–817, 2005.

[21] B. Palai, M. Biswal, S. Mohanty, and S. K. Nayak, "In situ reactive compatibilization of polylactic acid (PLA) and thermoplastic starch (TPS) blends; synthesis and evaluation of extrusion blown films thereof," *Industrial Crops and Products*, vol. 141, article 111748, 2019.

[22] W. Shujun, Y. Jiugao, and Y. Jinglin, "Preparation and characterization of compatible and degradable thermoplastic starch/polyethylene film," *Journal of Polymers and the Environment*, vol. 14, no. 1, pp. 65–70, 2006.

[23] C. L. Jun, "Reactive blending of biodegradable polymers: PLA and starch," *Journal of Polymers & the Environment*, vol. 8, no. 1, article 229248, pp. 33–37, 2000.

[24] A. Peacock, *Handbook of Polyethylene: Structures: Properties, and Applications*, CRC Press, 2000.

[25] H. G. Xiong, S. W. Tang, H. L. Tang, and P. Zou, "The structure and properties of a starch-based biodegradable film," *Carbohydrate Polymers*, vol. 71, no. 2, pp. 263–268, 2008.

[26] G. Giancola, R. L. Lehman, and J. D. Idol, "Melt processing and domain morphology of PMMA/HDPE polymer blends prepared from powder precursors," *Powder Technology*, vol. 218, pp. 18–22, 2012.

[27] J. B. Olivato, C. M. O. Müller, G. M. Carvalho, F. Yamashita, and M. V. E. Grossmann, "Physical and structural characterisation of starch/polyester blends with tartaric acid," *Materials Science and Engineering C*, vol. 39, no. 1, pp. 35–39, 2014.

[28] B. Zhang, X. Li, Q. Xie, H. Tao, W. Wang, and H. Chen, "Preparation and characterization of non-crystalline granular starch and corresponding carboxymethyl starch," *International Journal of Biological Macromolecules*, vol. 103, pp. 656–662, 2017.

[29] R. O. Sirotkin and N. W. Brooks, "The dynamic mechanical relaxation behaviour of polyethylene copolymers cast from solution," *Polymer*, vol. 42, no. 24, pp. 9801–9808, 2001.

[30] A. Pegoretti, M. Ashkar, C. Migliaresi, and G. Marom, "Relaxation processes in polyethylene fibre-reinforced polyethylene composites," *Composites Science and Technology*, vol. 60, no. 8, pp. 1181–1189, 2000.

[31] J. D. Hoffman, G. Williams, and E. Passaglia, "Analysis of the α, β, and γ relaxations in polychlorotrifluoroethylene and polyethylene: dielectric and mechanical properties," *Journal of Polymer Science Part C: Polymer Symposia*, vol. 14, no. 1, pp. 173–235, 1966.

[32] M. K. Abdul Wahab, H. Ismail, and N. Othman, "Compatibilization effects of PE-g-MA on mechanical, thermal and swelling properties of high density polyethylene/natural rubber/thermoplastic tapioca starch blends," *Polymer-Plastics Technology and Engineering*, vol. 51, no. 3, pp. 298–303, 2012.

[33] F. Yang, M. Zhang, J. G. Shi, W. W. Yu, X. R. Zou, and W. B. Zhou, "Study on the structure and properties of HDPE/starch composite for fishing," *Journal of Fisheries of China*, vol. 43, no. 11, pp. 2431–2437, 2019.

[34] A. Sharif, J. Aalaie, H. Shariatpanahi, H. Hosseinkhanli, and A. Khoshniyat, "Study on the structure and properties of nanocomposites based on high-density polyethylene/starch blends," *Journal of Polymer Research*, vol. 18, no. 6, pp. 1955–1969, 2011.

[35] X. Ma, J. Yu, and J. F. Kennedy, "Studies on the properties of natural fibers-reinforced thermoplastic starch composites," *Carbohydrate Polymers*, vol. 62, no. 1, pp. 19–24, 2005.

[36] M. L. Méndez-Hernández, C. S. Tena-Salcido, Z. Sandoval-Arellano, M. C. González-Cantú, M. Mondragón, and F. J. Rodríguez-González, "The effect of thermoplastic starch on the properties of HDPE/TPS blends during UV-accelerated aging," *Polymer Bulletin*, vol. 67, no. 5, pp. 903–914, 2011.

[37] V. O. Bulatović, D. K. Grgić, M. Slouf, A. Ostafinska, J. Dybal, and A. Jozinović, "Biodegradability of blends based on aliphatic polyester and thermoplastic starch," *Chemical Papers*, vol. 73, no. 5, pp. 1121–1134, 2019.